Proceedings of the ASME 2010 3rd Joint US-European Fluids Engineering Summer Meeting and 8th International Conference on Nanochannels, Microchannels, and Minichannels
FEDSM-ICNMM2010
August 1-5, 2010, Montreal, Canada

FEDSM-ICNMM2010-30834

Predictions of Turbulence Intensity in a Combustor Model Using Neural Network Analysis

Saad A. Ahmed and Hany El Kadi
College of Engineering, Mechanical Engineering Department,
American University of Sharjah, Sharjah, PO Box 26666, UAE
Phone: +971 6 5152468; Fax: +971 6 5152979
E-mail: sahmed@aus.edu

ABSTRACT

Predictions of turbulence intensity and continuous evolution of fluid flow characteristics in a combustor model are useful and essential for better and optimum design of gas turbine combustors. Many experimental techniques such as Laser Doppler Velocimetry (LDV) measurements provide only limited discrete information at given points; especially, for the cases of complex flows such as dump combustor swirling flows. For this type of flow, usual numerical interpolating schemes appear to be unsuitable. Neural Network Analysis (ANN) is proposed and the results are presented in this paper and are compared with the experimental data used for training purposes. This pilot study showed that artificial neural network is an appropriate method for predicting swirl flow characteristics in a model of a dump combustor. These techniques are proposed for better designs and optimization of dump combustors.
Keywords: Swirl Flow, dump combustors and Neural Network.

I. INTRODUCTION

Turbulent swirling flows are encountered in many engineering applications. For example, swirl is commonly employed in combustion systems (i.e.; gas turbines and ram jet engines) and also many chemical processing plants, in order to increase fluid mixing, heat and mass transfer rates, and subsequently improve the efficiency or the degree of stability of a process. Turbulent swirling flows have highly complex flowfields which are three-dimensional, unsteady and have reverse flow regions. They are also the subject of many experimental, numerical and theoretical investigations and have been reviewed extensively in the literature during the last five decades (i.e., see references 1-12).

Turbulent swirling flows remains a challenge in fluid mechanics and a large body of literature has been published dealing with various flow configurations (confined and unconfined, reacting and non-reacting) and/or specific phenomena such as flow structure and instabilities, and/or vortex breakdown. A comprehensive treatment on swirl flows can be found in the book by Gupta et al. (1984).

The axisymmetric sudden expansion geometry is relevant to many swirling applications, particularly swirl burners and combustors. Sudden expansion flows combine geometric simplicity with complex flow features such as separation and reattachment. They share many similarities with the flow past a backward facing step (i.e., the existence of three distinct flow regions: recirculation, reattachment and redevelopment). The reverse flow region size is an important feature of sudden expansion flows and it depends on swirl strength and type (i.e., free/forced vortex or constant angle), Reynolds number, expansion ratio, and free stream turbulence (i.e., see references 3-10).

The structure of swirling flows is very sensitive to the way the swirl is introduced, i.e., the inlet conditions. The effects of inlet or initial swirl profile and expansion angle on the characteristics of the swirling flow were investigated by Nejad and Ahmed (1992). Hallett and Toews (1987) showed that a lower velocity near the axis or a reduced radius of the solid body vortex core in the inlet will reduce the critical number required for central recirculation. An increase in the expansion ratio up to 1.5 will also reduce the critical swirl number. For expansion ratios greater than 1.5, either a reduction or an increase of the critical swirl number is reported, depending on inlet conditions. Nejad and Ahmed (1992) introduced swirl by three different types of swirlers: free vortex, forced vortex and constant angle, respectively. They showed that there are significant differences in the flowfield and turbulence characteristics when a different swirler is employed. In their study, for the same swirl number, a central recirculation was only observed in the case of free vortex type of swirling flow after the expansion. However, the centreline turbulence levels were the greatest for constant-angle swirling flow due to the large motion of the vortex centre precession.

The objective of the current study is to report detailed experimental database to help in the understanding of the behavior of axisymmetric, recirculating, and incompressible turbulent flows. There are two problems: (i) the obtained velocity-field is not continuous, (ii) the acquisition area remains limited and a complete investigation of the flowfield would request numerous measurement areas. Thus, an extensive experimental investigation would be expensive and require a very long time to obtain sufficient data. Since artificial neural networks (ANN) can deal with non-linear modeling, they seem to be an efficient tool for the reconstruction of data linked to multiple parameters, and thus an interesting alternative solution to common interpolation schemes. To evaluate the accuracy of this technique, a large set of data has first been measured using LDV technique. Next, the set has been divided into two parts: the first being used by the neural network in order to reconstruct the velocity-field during the learning step, and the second to estimate the reconstruction efficiency by comparing values obtained using ANN to experimental measurements.

NOMENCLATURE

H	step height, mm
M	sample size
R	combustor radius, mm
S	swirl number
U, V, W	mean velocity components, in x, r, and θ directions, m/s
u', v', w'	turbulence intensities of the velocity components, in x, r, and θ directions
U_o	mean axial reference velocity, upstream of the swirler, m/s
x, r, θ	axial, radial, and azimuthal coordinates; respectively, mm, mm, degrees

Greek Symbols

ρ	flow density, kg/m^3
ΔU	uncertainty in velocity U, m/s
μ	dynamic viscosity, Pa.s
σ_u	standard deviation of U, m/s

II. EXPERIMENTAL FACILITY AND INSTURMENTATION

2.1. Combustor Model

The experimental setup (Figure 1) consists of a movable swirler where the airflow enters the measurement section at ambient pressure and temperature (see Ahmed [10]). Special care was taken to ensure that the fabricated model satisfied the axisymmetric nature of the flowfield. The setup consisted of the inlet section and the combustion chamber.

The inlet section is made of a 300 *mm* diameter settling chamber, a plexiglas inlet pipe, and a cylindrical teflon swirler housing. The plexiglas inlet pipe is 2850 *mm* long and of 101.6 *mm* internal diameter while the teflon swirler housing has inner and outer diameters of 104.5 *mm* and 152.4 *mm*; respectively. The swirler housing has the ability of being positioned relative to the measurement station in the combustion chamber. This entire inlet assembly is placed on a traversing mechanism controlled by a stepping motor. The inlet flow measurements proved the inlet flow across the pipe to be a simple plug one. An average inlet velocity of 16.0 $\pm$ 0.4 *m/s* (large enough to ensure turbulent flow in the combustor, at a Reynolds number - based on the outer diameter of the swirler - of 1.5 x 10^5) was maintained throughout all experiments. This value of the inlet average velocity was checked with a flowmeter, located far upstream of the swirler housing.

The combustion chamber is made of a plexiglas tube, measuring 152.4 *mm* in diameter and 1850 *mm* in length. This section terminates into an exhauster of a larger diameter. The design of the test section also incorporates a plug assembly at the combustor exit that may be employed to increase the pressure of the chamber while keeping the mass flow rate unchanged. A 40 % contraction nozzle was situated at the combustor exit as part of the components of the flow facility to model the gas turbine combustor.

The swirler is a free vortex swirler which has 12 curved vanes. Swirler dimensions are 19 mm ID (central hub) and 101.6 mm OD.

2.2. Instrumentation

The velocity measurements in this study were done using a TSI Inc. 9100-7 four beam, two color, back scatter laser Doppler velocimeter LDV system. The LDV system had two TSI 9180-3A frequency shifters to provide directional sensitivity. A chemical seeder was developed and used for the present study. This chemical seeder produced micron size Titanium dioxide particles. These particles were injected into the upstream settling chamber in order to ensure that the flow was uniformly seeded.

The photomultipliers signals were processed by two TSI burst counters - models 1990 B\C with low pass filters, set at 20 MHz, and high pass filters set at 100 MHz on each processor. Calculations of statistical moments from standard formulae were done at each measurement location using double precision data (48 bit), see Ahmed [10]. The problem of velocity bias in LDV measurements was corrected in this study by the use of the time between individual realizations as a weighing factor (interarrival bias correction techniques), see Ahmed [10]. The uncertainty of the measured mean velocities was determined using the equation:

$$\Delta U = \pm 1.96 s_u / \sqrt{M}$$

The constant 1.96 is used for 95% confidence level, while M represents the sample size (i.e. 5000 for this study) and σ_u is the true standard deviation. The maximum uncertainties of the mean velocities U due to random errors were calculated and estimated to be 2.0 % of the upstream velocity U_o.

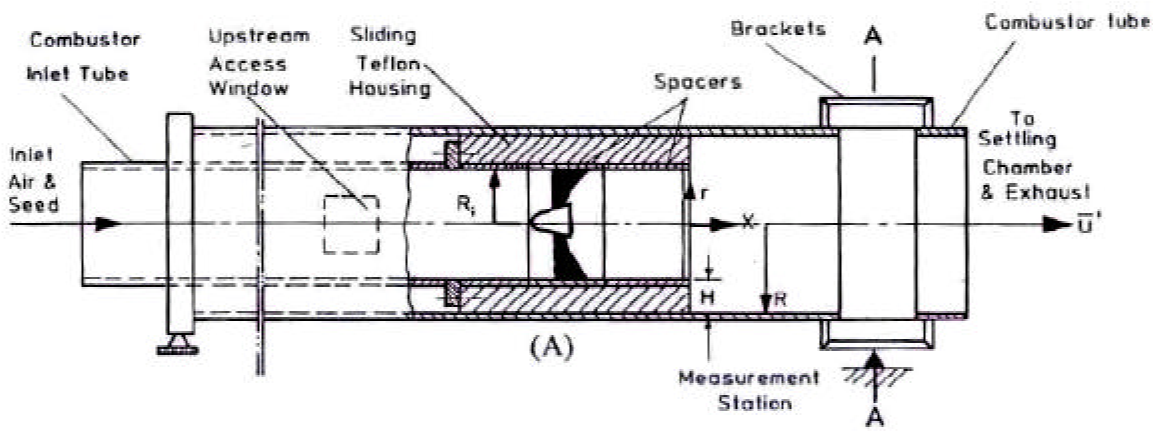

Fig. 1. Schematic of the dump combustor model

2.3. **ARTIFICAL NEURAL NETWORK**

Artificial neural networks (ANN) are computational systems that simulate the microstructure of a biological nervous system. The most basic components of ANNs are modeled after the structure of the brain for which the most basic element is a specific type of cell that provides us with the ability to remember, think and apply previous experience to our every action. These cells are known as neurons and each of these neurons can connect with hundreds of thousands of other neurons. The power of the brain comes from the number of these basic components and multiple connections between them.

Inspired by biological neurons, ANNs are composed of simple elements or artificial neurons operating in parallel to form a cluster of artificial neurons. The clustering is formed by creating layers connected to one another. As in nature, some of the neurons interface with the real world to receive its input (*input layer*), while others provide the world with the network's output (*output layer*). All remaining neurons are hidden (*hidden layers*). Each input to a neuron has a weight factor that determines the contribution of this neuron to the whole network.

Artificial Neural Networks are one of the artificial intelligence concepts that have proved to be useful in various engineering applications [11-23]. Their greatest advantage is in their ability to model complex non-linear, multi-dimensional functional relationships without any prior assumptions about the nature of the relationships and the network is built directly from experimental data by its self-organizing capabilities. The system can be considered as a black box and it is unnecessary to know the details of the internal behavior. These nets therefore may offer an accurate and cost effective approach for modeling engineering problems. ANN have already been used in medical applications, image and speech recognition, classification and control of dynamic systems, prediction of mechanical properties of materials among others; but only recently have they been used in swirl flow velocity field reconstruction [11-12].

The multilayered feed-forward neural network (FNN) is the most widely applied type of neural networks used by researchers so far. In general, feed-forward ANN consist of a layer of input neurons , a layer of output neurons and one or more layers of hidden neurons (Figure 2) [14, 15]. In the current work, the input parameters could be the *x, r* and *q* positions within the combustor where the turbulence intensity component is required and the output parameters could be the turbulence intensity component (s) to be predicted by the ANN at that specified position.

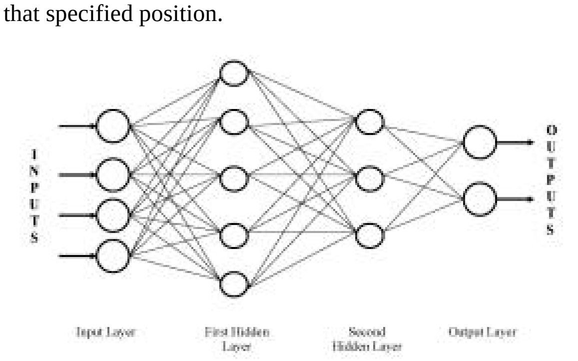

Fig. 2. General configuration of anartificial neural network [14]

A back-propagation algorithm can train the ANN with differentiable transfer functions. The term back propagation refers to the process by which derivatives of network error, with respect to network weights and biases, can be computed. The back-propagation training algorithm is commonly used to iteratively minimize the following cost function with respect to the interconnection weights and neurons thresholds:

$$E = \frac{1}{2} \sum_{1}^{P} \sum_{i=1}^{N} (d_i - O_i)^2$$

where P is the number of experimental data pairs used in training the network and N is the number of output parameters expected from the ANN. d_i and O_i could be one of the experimentally-measured turbulence intensity components of the flow and the ANN prediction of that component at a specific location i within the combustor, respectively.

The training process is terminated either when the Mean-Square-Error (*MSE*), Root-Mean-Square-Error (*RMSE*), or Normalized-Mean-Square-Error (*NMSE*), between the actual experimental results and the ANN predictions obtained for all elements in the training set has reached a pre-specified threshold or after the completion of a pre-specified number of learning epochs [14].

In mathematics and computing, the Levenberg-Marquardt (LM) algorithm is an iterative technique that locates the minimum of a multivariate function that is expressed as the sum of squares of non-linear real-valued functions [19, 20]. It has become a standard technique for non-linear least-squares problems, widely adopted in a broad spectrum of disciplines. LM can be thought of as a combination of the steepest descent and the Gauss-Newton methods. When the current solution is far from the correct one, the algorithm behaves like a steepest descent method: slow, but guaranteed to converge. When the current solution is close to the correct solution, it becomes a Gauss-Newton method. In this work, the LM algorithm will be used to train the feed-forward neural network used [21].

III. RESULTS AND DISCUSSION

A trained ANN can be thought of as an expert in the category of information it has been given to analyze. This expert can then be used to provide predictions given new situations of interest. In this study, the suitability of ANN to predict experimental results obtained at different locations will be investigated. The coordinates *x* and *r* will be used as the input parameters to the ANN while the turbulence intensities will be the output from the network. For this initial work, rather than having one complex neural network predicting all turbulence intensity components, a simpler network will be used to separately predict each of the components.

The Neurosolution-5 software [24] was used to construct, train and test the networks. In each case, the network was trained using all but one of the turbulence intensity distributions obtained experimentally at different values of the coordinate *x*. The network was then required to predict the profile it was not trained for. The predictions obtained were then compared to the experimental results at this coordinate. Once assured that the predictions obtained are reliable, the network could be used in the future to predict the turbulence intensity profile at any coordinate *x* for which experimental data do not exist. Since the ANN cannot be accurately used to predict results outside the area of training, predicting the profiles at x/H = 0.38 and x/H = 18 was not attempted.

In this investigation, the effect of the ANN architecture was not considered. This is because the main goal of this study is to establish the feasibility of using ANN to predict the turbulence intensities. In future studies, the effect of using different ANN architectures (such as Radial Basis Function, Modular, Self-Organizing and Principal Component Analysis) could be examined. The number of hidden layers was kept at one and the number of training epochs was held

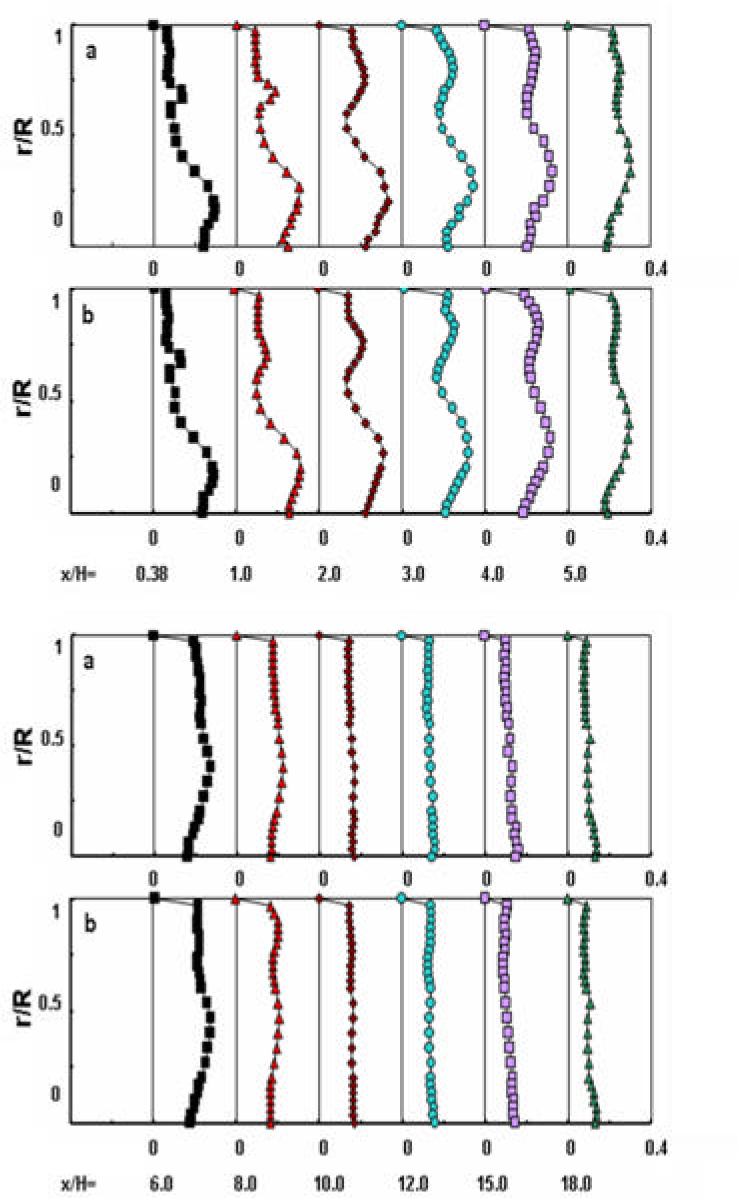

Fig. 3. **Evolution of axial turbulence intensity profiles, 0's indicate the origin for each profile. Top graphs have near field results and bottom graphs have mid and far field results. (a) Experimental results; (b) ANN results**

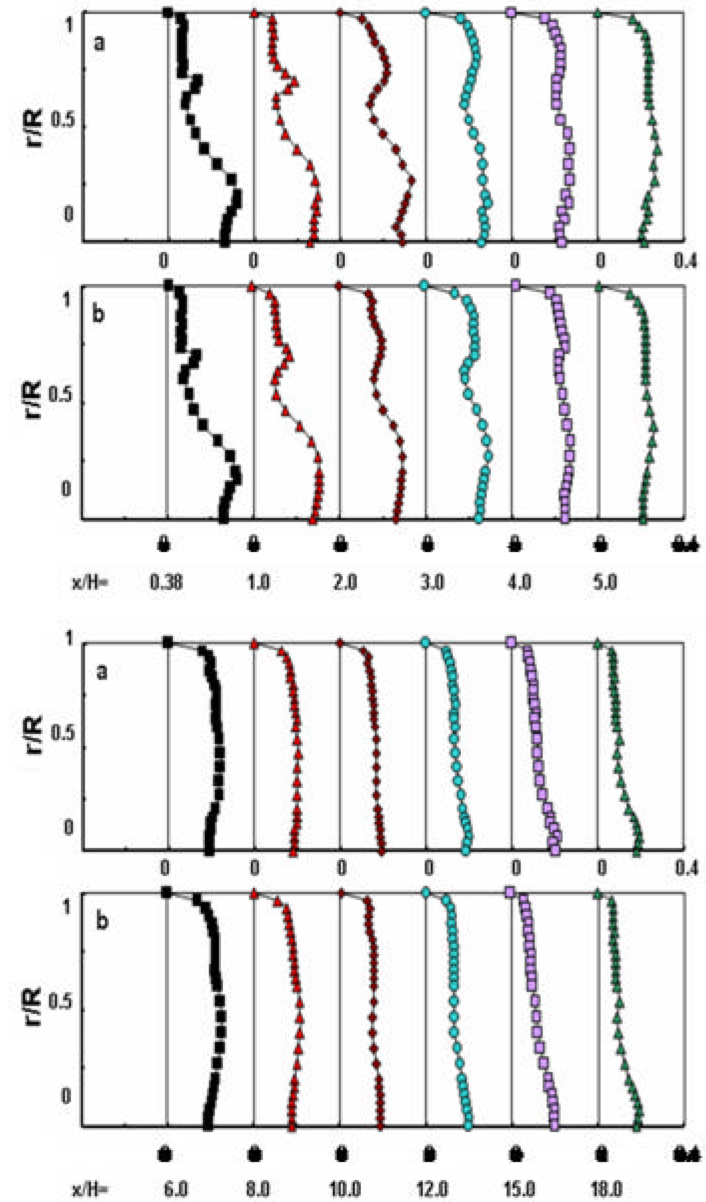

Fig. 4. **Evolution of radial turbulence intensity profiles, 0's indicate the origin for each profile. Top graphs have near field results and bottom graphs have mid and far field results. (a) Experimental results; (b) ANN results**

constant at 1000 epochs. To evaluate the accuracy of the neural network, the correlation coefficient (*cc*) and the normalized mean square error (*NMSE*) were calculated. Table 1 shows the *cc* and *NMSE* obtained for each of the turbulence intensity profiles considered. These results show that ANN can be used to accurately predict the turbulence intensities distributions in dump combustors.

The turbulence intensities distributions at various values of the distance x can be graphically represented. Figures 3 and 4 show the experimental and predicted turbulence intensities profiles in the axial and radial directions at x / H = 0.38, 1, 2, 3, 4, 5, 6, 8, 10, 12, 15 and 18; respectively. The predictions of the shear stresses are not shown here due to the paper's size limitation.

It is obvious that two peaks characterized the swirling flow around the inner and outer shear layers (i.e., the larger is seen in the boundaries of CTRZ, and the smaller occurred in the shear layer of CRZ). Turbulence activities are gradually reduced downstream of the reattachment point. It is interesting to note that the peak value of axial turbulence intensities is observed to move towards the combustor wall as it decays in strength and grows in size, indicating a progressive development of the outer shear layer. Turbulence activity is seen to be more concentrated in the central shear layer and the centers of the maximum values, for the two regions are located approximately at x / H = 3.0 .

Table 1. Correlation coefficient (*cc*) and normalized mean square error (*NMSE*) as a function of *x/H*

x/H	*u'*		*v'*		*w'*	
	cc	NMSE	cc	NMSE	cc	NMSE
1.0	0.9765	0.05820	0.9911	0.02940	0.9824	0.05915
2.0	0.9846	0.05297	0.9789	0.05486	0.9750	0.09690
3.0	0.9715	0.06285	0.9752	0.05439	0.9728	0.07211
4.0	0.9785	0.04866	0.9835	0.07464	0.9532	0.11042
5.0	0.9774	0.06406	0.9905	0.08305	0.9883	0.03645
6.0	0.9855	0.05516	0.9874	0.03764	0.9680	0.06379
8.0	0.9327	0.13788	0.9824	0.03885	0.9745	0.12272
10.0	0.9745	0.07873	0.9806	0.04465	0.9717	0.26279
12.0	0.9578	0.10975	0.9918	0.01707	0.9772	0.07506
15.0	0.9789	0.07534	0.9918	0.05688	0.9635	0.30149

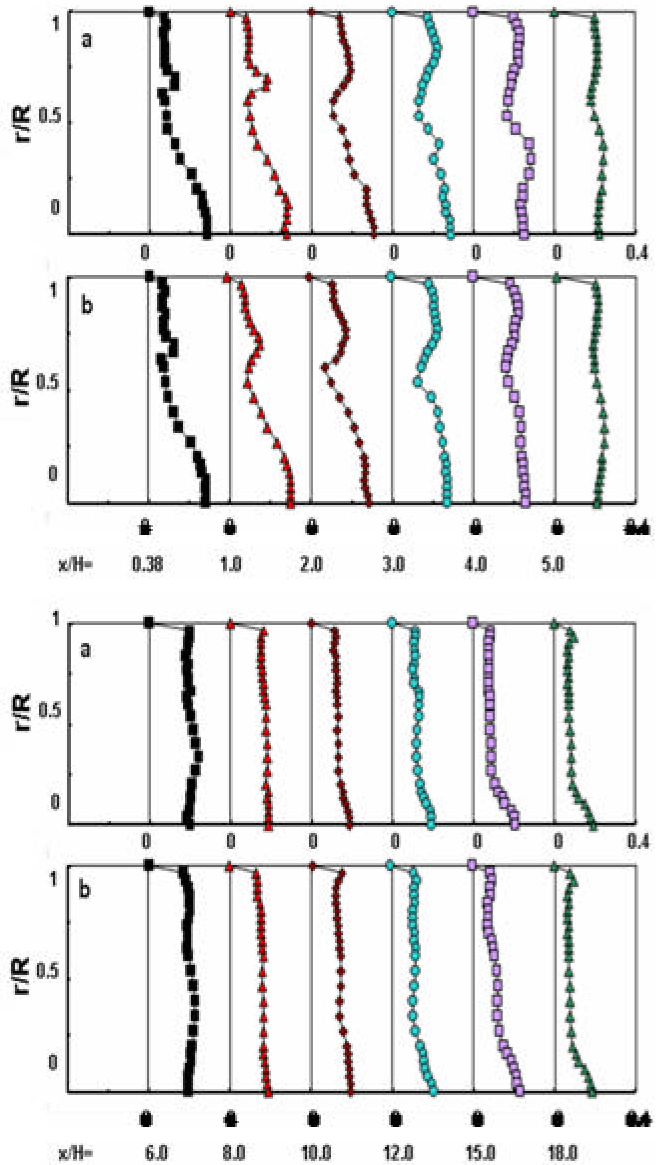

Fig. 5. Evolution of tangential turbulence intensity profiles, 0's indicate the origin for each profile. Top graphs have near field results and bottom graphs have mid and far field results. (a) Experimental results; (b) ANN results

The features of the tangential turbulence intensities (see Fig. 5) are similar to those described above for the axial turbulence intensities. Near the core, the flow did not recover completely (due to the existence of CTRZ) as indicated by relatively higher values of stresses at each axial location, and downstream of $x / H = 10$.

IV. CONCLUSIONS

A two component LDV system was utilized to measure the turbulence intensities flowfield characteristics of a free vortex swirler. As a result, a database of the flowfield characteristics was established over a fairly wide region, *0.38H* to *18H* downstream of the step including the regions of major interest (i.e., corner recirculation and central toroidal recirculation zones). The swirler reduced the flow reattachment point considerably. As a result, turbulent flow recovers shortly after the reattachment point in a short distance enhancing combustion characteristics. Furthermore, energy is distributed on both sides of the shear layer in the region close to the centerline of the combustor and flow separation areas. Thus, it is obvious that a swirler in the combustor will have important effects on the flow characteristics. This detailed information should be of value for further development of second order closure models.

A comparison between the experimental data and the turbulence intensity predictions using ANN reveals high correlation. These observations are obvious from the results reported in Table 1 as well as Figures 3-5. These encouraging results show the suitability of the ANN as a method for predicting the swirl flow turbulence characteristics reconstruction and warrant proceeding with the prediction of the normal and shear stresses of all velocity components. More work is underway to show the applicability to higher order turbulence statistics as well as the effect of the ANN architecture on the predicted values.

ACKNOWLEDGEMENTS

The authors wish to acknowledge the support of AUS for utilizing the various facilities in preparation of the manuscript.

REFERENCES

[1] Buckley, P.L., Craig, R.R., Davis, D.L. and Schwartzkopf, K.G., 1983 "The Design and Combustion Performance of Practical Swirlers for Integral Rocket / Ramjets," AIAA Journal, Vol. 21, No. 5, pp. 743-740.

[2] Gupta, A.K., and Lilley, D.G., 1984 "Flowfield Modeling and Diagnostics" Abacus Press, Turnbridge Wells, UK.

[3] Dong, M., and Lilley, D.G., 1994 "Inlet Velocity Profile Effects on Turbulent Swirling Flow Predictions," Journal of Propulsion and Power, Vol. 10, No. 2, pp 155-160.

[4] Nejad, A.S., Ahmed, S.A., 1992. "Flow field characteristics of an axisymmetric sudden-expansion pipe flow with different initial swirl distribution, " International Journal of Heat and Fluid Flow, 13, 314–321.

[5] Hallett, W.L.H., Toews, D.J., 1987 "The effect of inlet conditions and expansion-ratio on the onset of flow reversal in swirling flow in a sudden expansion, "Experiments in Fluids, 5 (2), 129–133.

[6] Tinney, C.E., Glauser, M.N., Eaton, E.L., Taylor, J.A., 2006 "Low dimensional azimuthal characteristics of suddenly expanding axisymmetric flows, " Journal of Fluid Mechanics, 567, 141–155.

[7] Wang, P., Bai, X.S., Wessman, M., Klingmann, J., 2004 "Large eddy simulation and experimental studies of a confined turbulent swirling flow," Physics of Fluids 16 (9), 3306–3324.

[8] Zhou, L.X., Li, Y., Chen, T., Xu, Y., 2000 "Studies on the effect of swirl numbers on strongly swirling turbulent gas–particle flows using a phase-Doppler particle anemometer," Powder Technology 112, 79–86.

[9] Vanka, S.P., Krazinski, J.L., and Nejad, A.S., 1988 "An Efficient Computational Tool for Ramjet Combustor Research," AIAA Paper No. 88-0060.

[10] Ahmed, S.A., 1998 "Velocity measurements and turbulence statistics of a confined isothermal swirling flow," Experimental Thermal and Fluid Science Journal, Vol. 17, pp. 256-264.

[11] Pruvost, J., Legrand, J., and Legentilhomme, P., 2001 "Three dimensional swirl flow velocity-field reconstruction using a neural network with radial basis function," Transaction of the ASME – Journal of Fluids Engineering, vol. 123, pp. 920-927.

[12] Ghorbanian, K., Soltani, M.R., Morad, M.R., and Ashjaee, M., 2005 "Velocity field recognition in the mixing region of swirl sprays using general regression neural networks," Transaction of the ASME – Journal of Fluids Eng., vol. 127, pp. 14-23.

[13] Haykin S., 1993 "Neural Networks for statistical modeling. Van Nostrand Reinhold Editor.

[14] El Kadi, H., 2006 "Modeling the Mechanical Behavior of Fiber-Reinforced Polymeric Composite Materials Using Artificial Neural Networks – A Review." Composite Structures 73, pp 1-23.

[15] Skapura D., 1996 "Building Neural Networks". ACM Press, Addison-Wesley Publishing Company, New York.

[16] Herzallah R, Al-Assaf Y., 2000 "Control of non-linear and time-variant dynamic systems using neural networks," Proceedings of the 4th World Multiconference on SYSTEMICS, CYBERNETICS and INFORMATICS, Florida.

[17] Mansoor W, Al-Nashash H, Al-Assaf Y., 2000 "Image classification using wavelets and neural networks," The 18th IASTED International Conference on Applied Informatics, Innsbruck, Austria.

[18] Al-Assaf, Y., El Kadi, H., 2001 "Fatigue Life Prediction of Unidirectional Glass Fibre/Epoxy Composite Laminae using Neural Networks," Composite Structures, vol. 53, pp. 65-71.

[19] Levenberg, K., 1944 "A Method for the Solution of Certain Non-linear Problems in Least Squares," Quarterly of Applied Mathematics, 2(2):164–168.

[20] Marquardt, D.W., 1963 "An Algorithm for the Least-Squares Estimation of Nonlinear Parameters," SIAM Journal of Applied Mathematics, 11(2):431–441.

[21] Hagan, M.T. and Menhaj, M., 1994 "Training feed-forward networks with the Marquardt algorithm," IEEE Transactions on Neural Networks, vol. 5, pp.989-993.

[22] Rosenblatt, F., 1962 "Principles of neurodynamics," Spartan Books, Washington DC.

[23] Kohonen, T., 1984 "Self-organization and associative memory," Springer-Verlag. Berlin.

[24] Neurosolutions 5 software, 2005: www.nd.com